

## ORIGINAL ARTICLE

# Polythiophene nanoparticles that display reversible multichromism in aqueous media

Krishnachary Salikolimi<sup>1,2</sup>, Masuki Kawamoto<sup>1,3,4</sup>, Pan He<sup>1</sup>, Toshiro Aigaki<sup>2</sup> and Yoshihiro Ito<sup>1,2,3</sup>

Conjugated polymer nanoparticles in aqueous media have received much attention because of their specific electronic, optical and medicinal properties. However, flexible hydrophilic chains such as oligo(ethylene oxide) groups on the outer surface of the nanoparticles may induce increases in the particle size resulting from the aggregation of nanoparticles in water. We designed a bolaamphiphilic monomer to produce polythiophene nanoparticles. The resulting nanoparticles exhibit multichromic responses to solvent, temperature and acid/base that can be detected by the naked eye. The nanoparticles, with an average diameter of 170 nm and a large zeta potential of –66.6 mV, remain stable in tetrahydrofuran/water mixtures even after 8 months. As the concentration of water increases, the nanoparticles turn from yellow to violet because the molecular conformation of the thiophene units changes. The nanoparticles dispersed in water display a reversible thermochromic response between 20 and 90 °C, which originates from their different morphologies of an amorphous solid below and an isotropic liquid above their melting point of 60 °C. Adding hydrobromic acid yields an almost colorless dispersion because of the formation of polarons (p-doping), and the nanoparticles revert to their initial violet dispersion upon bubbling with ammonia gas owing to the dedoping of the polythiophene nanoparticles.

*Polymer Journal* (2017) 49, 429–437; doi:10.1038/pj.2017.5; published online 22 February 2017

## INTRODUCTION

Conjugated polymers have emerged as promising candidates for functional materials.<sup>1,2</sup> Molecular design enables precise control over supramolecular self-assembly and molecular organization to focus on modulating the electronic and optical properties.<sup>3</sup> Chromic responses are among the most promising molecular functions of conjugated polymers.<sup>4</sup> Intriguing changes in color, such as solvatochromism and thermochromism, have been observed in polydiacetylenes,<sup>5,6</sup> polythiophenes<sup>7,8</sup> and polyfluorenes.<sup>9,10</sup> Color modulation of conjugated polymers is affected by the conjugation length in their main chain. When chain planarization and concomitant interchain  $\pi$ -stacking occur in a poor solvent or at low temperature, an increase in the conjugation length can be obtained at the molecular level, resulting in a color change.

Recently, conjugated polymer nanoparticles in aqueous media have attracted particular interest because of the specific behavior arising from their self-assembled nanostructures.<sup>11,12</sup> Because they are semi-conducting, fluorescent and non-toxic, these nanomaterials are attractive for optoelectronic,<sup>13</sup> bioimaging<sup>14–16</sup> and nanomedical<sup>17,18</sup> applications. Solubilizing side chains are required to form conjugated polymer nanoparticles. Because their rigid conjugated main chain results in low solubility in organic solvents, the unsubstituted polymers are insoluble in many solvents. Ethylene oxide groups have been used

as solubilizing hydrophilic side chains to obtain self-assembled nanoparticles in aqueous media.<sup>19,20</sup> These nanoparticles consist of conjugated polymers synthesized from amphiphilic monomers. Sometimes the flexible ethylene oxide groups give rise to instability, such as the aggregation of the nanoparticles in water.<sup>21</sup> We assumed that if a nanoparticle is covered with less flexible ethylene oxide chains, a stable nanostructure could be maintained. To realize this strategy, we design a bolaamphiphilic monomer consisting of thiophene, oligo(ethylene oxide) and phenyl groups (Figure 1). The self-assembled aggregation between hydrophobic thiophene and phenyl groups is expected to occur in aqueous media. In this study, we use octylphenol ethoxylate as a side chain in the bolaamphiphilic monomer. Octylphenol ethoxylate is a nonionic surfactant that is widely used in pharmacy and medicine<sup>22–24</sup> because it induces the solubilization and dissociation of hydrophobic proteins, such as enzymes and receptors, to yield spherical or cylindrical micelles in water. From the viewpoint of side-chain engineering,<sup>25</sup> a terminal octylphenol ethoxylate group that is directly connected to a hydrophobic polythiophene moiety may promote nanoparticle formation.

The formation of conjugated polymer nanoparticles in aqueous media involves competition between interchain aggregation and intrachain collapse in the conjugated polymers, and the interfacial surface tension between the polymer and water may dominate.<sup>26,27</sup>

<sup>1</sup>Emergent Bioengineering Materials Research Team, RIKEN Center for Emergent Matter Science, RIKEN, Saitama, Japan; <sup>2</sup>Department of Biological Sciences, Tokyo Metropolitan University, Tokyo, Japan; <sup>3</sup>Nano Medical Engineering Laboratory, RIKEN, Saitama, Japan and <sup>4</sup>Photocatalysis International Research Center, Tokyo University of Science, Chiba, Japan

Correspondence: Dr M Kawamoto or Dr Y Ito, Emergent Bioengineering Materials Research Team, RIKEN Center for Emergent Matter Science, RIKEN, W502, Cooperation Center Building, 2-1 Hirosawa, Wako, Saitama 351-0198, Japan.

E-mail: mkawamoto@riken.jp or y-ito@riken.jp

Received 19 December 2016; revised 15 January 2017; accepted 15 January 2017; published online 22 February 2017

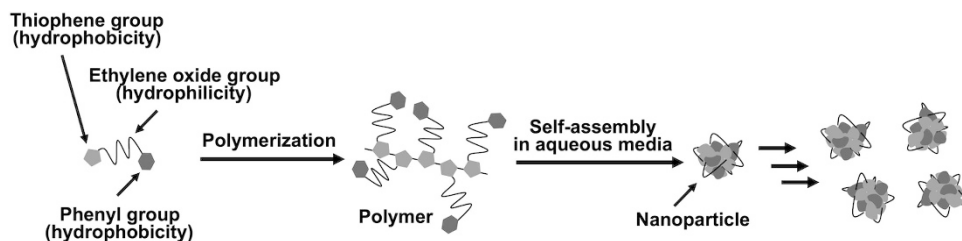


**Figure 1** Schematic illustration of the formation of polythiophene nanoparticles from bolaamphiphilic monomers.

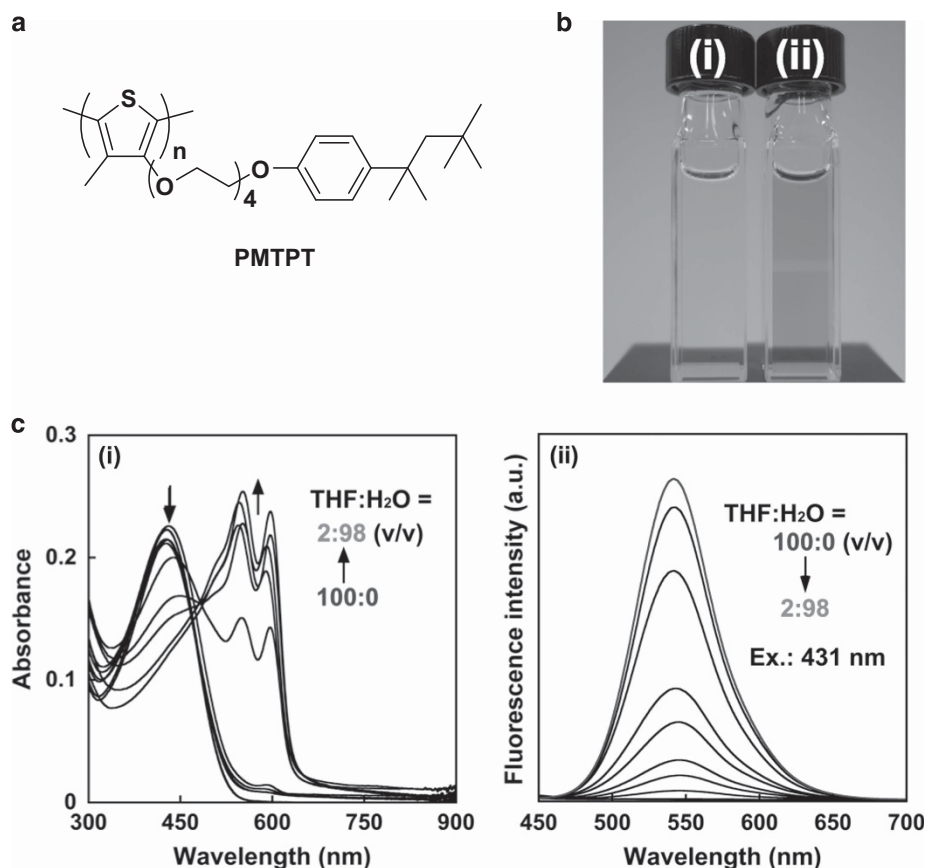


**Figure 2** (a) Molecular structure of **PMTPT**. (b) Photographs of (i) **PMTPT** in THF and (ii) **PMTPT** nanoparticles in THF:H<sub>2</sub>O = 2:98 (v/v) under irradiation at 633 nm by a HeNe laser beam. (c) Changes in (i) absorption and (ii) fluorescence spectra of the **PMTPT** nanoparticles with water concentration. Excitation wavelength (Ex.): 431 nm. THF, tetrahydrofuran.

We expected that if the morphological properties of the nanoparticles are controlled by external stimuli, the dynamic modulation of the molecular conjugation in aqueous media could occur. In this article, we demonstrate that the polythiophene derivative obtained from the bolaamphiphilic monomer forms self-assembled nanoparticles that show multichromic behavior including solvatochromism and thermochromism in tetrahydrofuran (THF)/water mixtures. The nanoparticle color can be tuned from yellow to violet by varying the water concentration. A thermochromic response is observed because the nanoparticles can adopt different molecular confirmations without deformation or aggregation. Furthermore, the nanoparticles display halochromic behavior in aqueous dispersions upon alternately adding hydrobromic acid and ammonia gas. This halochromic response also leads to a change in electrical conductivity in the solid state, resulting from the chemical doping of the conjugated main chain.

## MATERIALS AND METHODS

### Sample preparation

The nanoparticles in THF/water mixtures with various ratios were prepared as follows. First, the polymer (**PMTPT**) in THF (2.5 mg l<sup>-1</sup>) was added to specific volumes of THF to afford mother solutions of various concentrations. Each mother solution was injected into certain volumes of water to immediately yield **PMTPT** nanoparticle solutions without applying a mechanical force such as stirring or ultrasonication. For example, **PMTPT** nanoparticles in THF:H<sub>2</sub>O (3 ml, 2:98 v/v) was prepared by injecting a THF solution of **PMTPT** (60 µl, 2.5 mg l<sup>-1</sup>) into water (2.94 ml). A similar method was used to afford the nanoparticles in THF/EtOH mixtures. Thin films of **PMTPT** were fabricated by spin-coating chloroform solutions of the polymer (1 wt%) onto fused silica substrates at a rate of 2000 r.p.m. for 30 s and annealing the films at 60 °C for 15 min. Samples for the electrical conductivity measurements were prepared by casting **PMTPT** solution (1 wt%) on interdigitated gold electrodes (BAS, Inc., Tokyo, Japan) consisting of 130 gold fingers with a length of

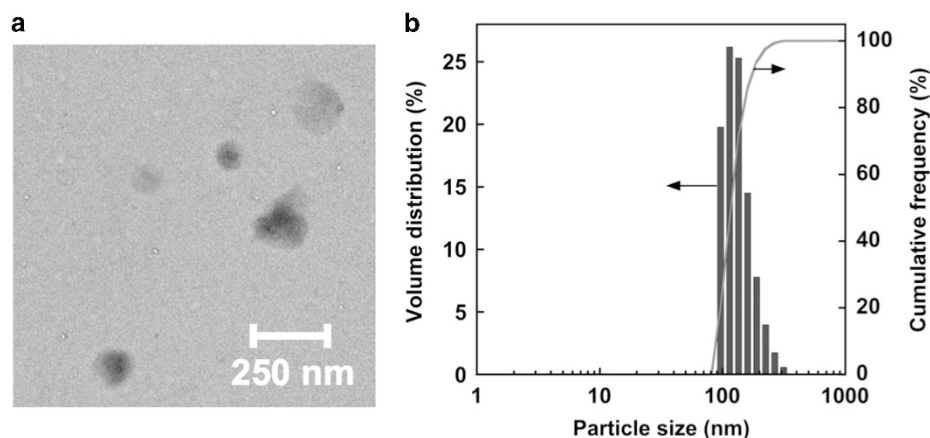


**Figure 3** (a) TEM image of the **PMTPT** nanoparticles. (b) Size distribution of the **PMTPT** nanoparticles in THF:H<sub>2</sub>O = 2:98 (v/v). TEM, transmission electron microscopy; THF, tetrahydrofuran.

2.4 mm, width of 10  $\mu$ m, height of 90 nm and gap between fingers of 5  $\mu$ m, followed by drying under reduced pressure before measurement.

## RESULTS AND DISCUSSION

### Synthesis and characterization of PMTPT

Figure 2a shows the molecular structure of the polymer (**PMTPT**) obtained from the bolaamphiphilic monomer; full synthetic details are provided in the Supplementary Information. To obtain **PMTPT**, methoxylated thiophene **1** was conveniently prepared by reacting 3-bromo-4-methylthiophene with sodium methoxide. The nucleophilic substitution of 4-(1,1,3,3-tetramethylbutyl)phenol with tosylated tetraethylene glycol afforded terminal group **3**. Bolaamphiphilic monomer **4** was synthesized by a conventional ether reaction between **1** and **3**. The oxidation coupling of **4** using iron(III) chloride produced the target polymer **PMTPT**. The polymer was successfully purified using size-exclusion chromatography to remove oligomers and impurities. We analyzed the <sup>1</sup>H NMR spectra of **PMTPT** to evaluate the integration of the side chains because oxidative polymerization may result in the oxidation of the ethylene oxide groups (Supplementary Figure S1B).<sup>28</sup> The integration of the oligoethylene oxide groups (peaks b and c) in the side chain was consistent with 16 protons. In contrast, the integration of the methyl group in the thiophene ring (peak c) was consistent with three protons (Supplementary Figure S1A). Judging from the <sup>1</sup>H NMR spectra of monomer **4** and **PMTPT**, appreciable degradation did not occur under the polymerization conditions used. The number-average molecular weight ( $M_n$ ) and polydispersity (weight-average molecular weight ( $M_w/M_n$ )) of **PMTPT** were 40 500 and 1.90, respectively, at 25 °C. The thermal behavior of **PMTPT** was investigated by thermogravimetric analysis and differential scanning calorimetry (DSC). Thermogravimetric analysis indicated that **PMTPT** had lost 10% of its weight at 325 °C (Supplementary Figure S2A). We also detected endothermic events for **PMTPT** corresponding to a glass transition temperature ( $T_g$ ) of -10 °C and melting point ( $T_c$ ) of 60 °C [change in enthalpy ( $\Delta H$ ): 6.3 kJ mol<sup>-1</sup>] on the third cycle in DSC measurements (Supplementary Figure S2B). **PMTPT** was readily soluble in THF, chloroform and DMF (*N,N*-dimethylformamide) but insoluble in water, acetone and alcohols.

### Solvatochromic behavior

The maximum absorption wavelength  $\lambda_{\max}$  of **PMTPT** in THF was 431 nm, which was attributed to a  $\pi$ - $\pi^*$  transition of the

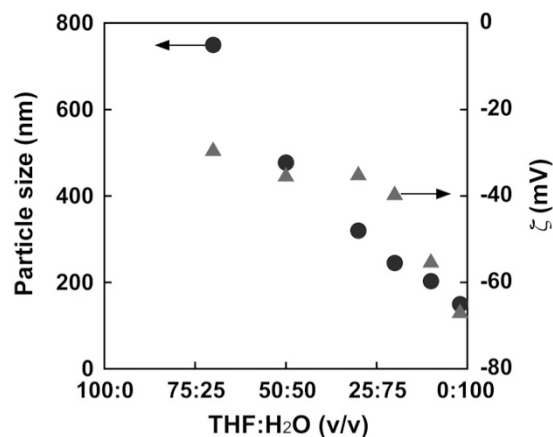


**Figure 4** Relationship between particle size and zeta potential ( $\zeta$ ) of **PMTPT** in solutions with various concentrations of THF and H<sub>2</sub>O. THF, tetrahydrofuran.

polythiophene units arising from a random coil conformation in the polymer backbone.<sup>29</sup> No marked change in  $\lambda_{\max}$  occurred in chloroform (429 nm) or DMF (445 nm; Supplementary Figure S3A). The polymer displayed yellow fluorescence in THF, with an emission peak at 542 nm (excitation wavelength: 431 nm). The fluorescence quantum yield of **PMTPT** in THF, determined using fluorescein as a standard, was 8%.<sup>30</sup>

As the concentration of water in the solution mixtures was increased, the color clearly changed from yellow to violet (Figure 2b and Supplementary Figure S8A). **PMTPT** in THF:H<sub>2</sub>O (2:98 v/v) formed a colloidal dispersion, as evidenced by the light scattering of a 633 nm laser beam. Unfortunately, the formation of a violet precipitate of **PMTPT** occurred in pure water after the evaporation of THF from the THF/water mixtures. Figure 2c-(i) shows changes in the absorption spectra of **PMTPT** at various concentrations of water. As the water content increased, the absorbance at 431 nm decreased and new absorption peaks appeared at 552 and 598 nm. These new absorption bands are assigned to the vibronic propagation of the  $\pi$ - $\pi^*$  transition in the polymer main chain, and  $\lambda_{\max}$  depends on the conformation of the polythiophene groups. **PMTPT** with a  $\lambda_{\max}$  of approximately 430 nm has a nonplanar conformation with less conjugation. In contrast, the absorption peaks at approximately

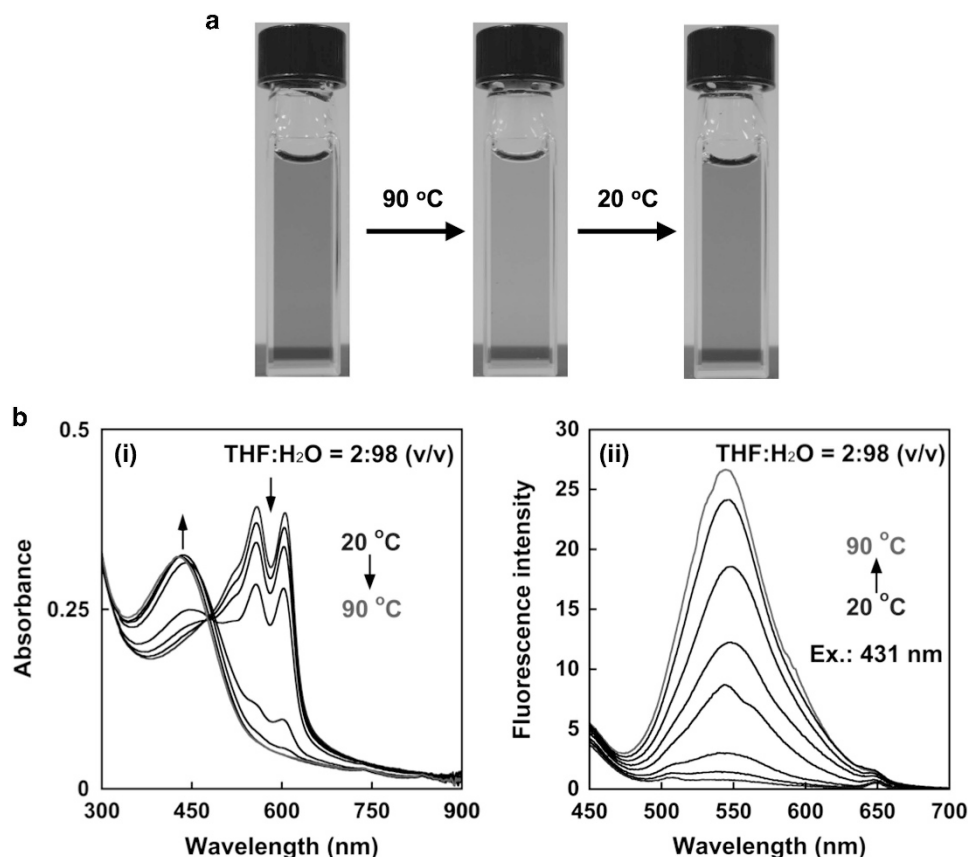


**Figure 5** (a) Thermochromic behavior of **PMTPT** nanoparticles in THF:H<sub>2</sub>O=2:98 (v/v) between 20 and 90 °C. (b) Changes in (i) absorption and (ii) fluorescence spectra of **PMTPT** nanoparticles in THF:H<sub>2</sub>O=2:98 (v/v) upon heating. Excitation wavelength (Ex.): 431 nm. THF, tetrahydrofuran.

550–600 nm originate from a planar conformation with an extended conjugated structure.<sup>31</sup> **PMTPT** in a neat film (Supplementary Figure S3B) exhibited similar absorption peaks to the **PMTPT** nanoparticles in THF:H<sub>2</sub>O (2:98 v/v). We also found that an isosbestic point at 486 nm was observed when the concentration was above 50 volume percent of water. This indicates that the molecular conformation of **PMTPT** is affected by changes in the concentration of water.

We assume that the modulation of the absorption spectra is caused by the polymer assembly in aqueous media, which leads to a planar organization of the polythiophene units. The formation of the assembled structure was also observed as changes in the fluorescence spectra (Figure 2c-(ii)). As mentioned above, **PMTPT** exhibited yellow fluorescence in THF following excitation at 431 nm. The fluorescence intensity gradually decreased with the increasing water concentration. In THF:H<sub>2</sub>O (2:98 v/v), the fluorescence intensity of **PMTPT** was almost negligible. These results also suggest that fluorescence quenching is caused by the formation of the assembled structure with planar polythiophene units in aqueous media.

To clarify the assembly behavior of **PMTPT** in aqueous media, structural examination was performed by transmission electron microscopy (TEM). TEM samples were prepared by pipetting a few microliters of the **PMTPT** solution in THF:H<sub>2</sub>O (2:98 v/v) onto a TEM grid. TEM analysis revealed the formation of colloidal nanoparticles with an average size of ~150 nm (Figure 3a). To determine the size distribution of the **PMTPT** nanoparticles, dynamic light scattering (DLS) measurements were conducted (Figure 3b).

A narrow particle size distribution was obtained: all the particles were in the range from 100 to 300 nm, and the average particle size was 168 nm with a polydispersity index of 0.07. The average particle size determined by DLS was similar to that observed by TEM. Furthermore, the dispersed nanoparticles were negatively charged, with a high zeta potential ( $\zeta$ ) of -66.6 mV. The stability of the nanoparticles was investigated; they displayed an average particle size of 190 nm with a polydispersity index of 0.12 following standing for 8 months (Supplementary Figure S4). The  $\zeta$  value of the nanoparticles was -81.9 mV after 8 months, revealing that the aqueous dispersion of **PMTPT** nanoparticles was stable without precipitation because of the electrostatic repulsion induced by their highly negative surface charge. The observation of the stable and high  $\zeta$  value is still unclear at the present stage. The introduction of negatively charged carboxylic acid<sup>32</sup> and sulfonate<sup>33</sup> leads to an electrical double layer with a high negative  $\zeta$  value. In contrast, **PMTPT** is a neutral polymer without the charged group. One possibility is that the self-assembled aggregation between hydrophobic thiophene and phenyl groups may contribute to the formation of the stable charge at the surface of the nanoparticle. Furthermore, the hydrophilic oligo(ethylene oxide) group in the outer part of the nanoparticle is crucial for the formation of a stable dispersion in aqueous media.

Next, the relationship between the particle size and water concentration was investigated (Figure 4). **PMTPT** nanoparticles with a particle size of 750 nm were observed when THF:H<sub>2</sub>O=75:25 (v/v). The particle size clearly decreased with the increasing water concentration in the mixtures. In contrast, the  $\zeta$  values became more

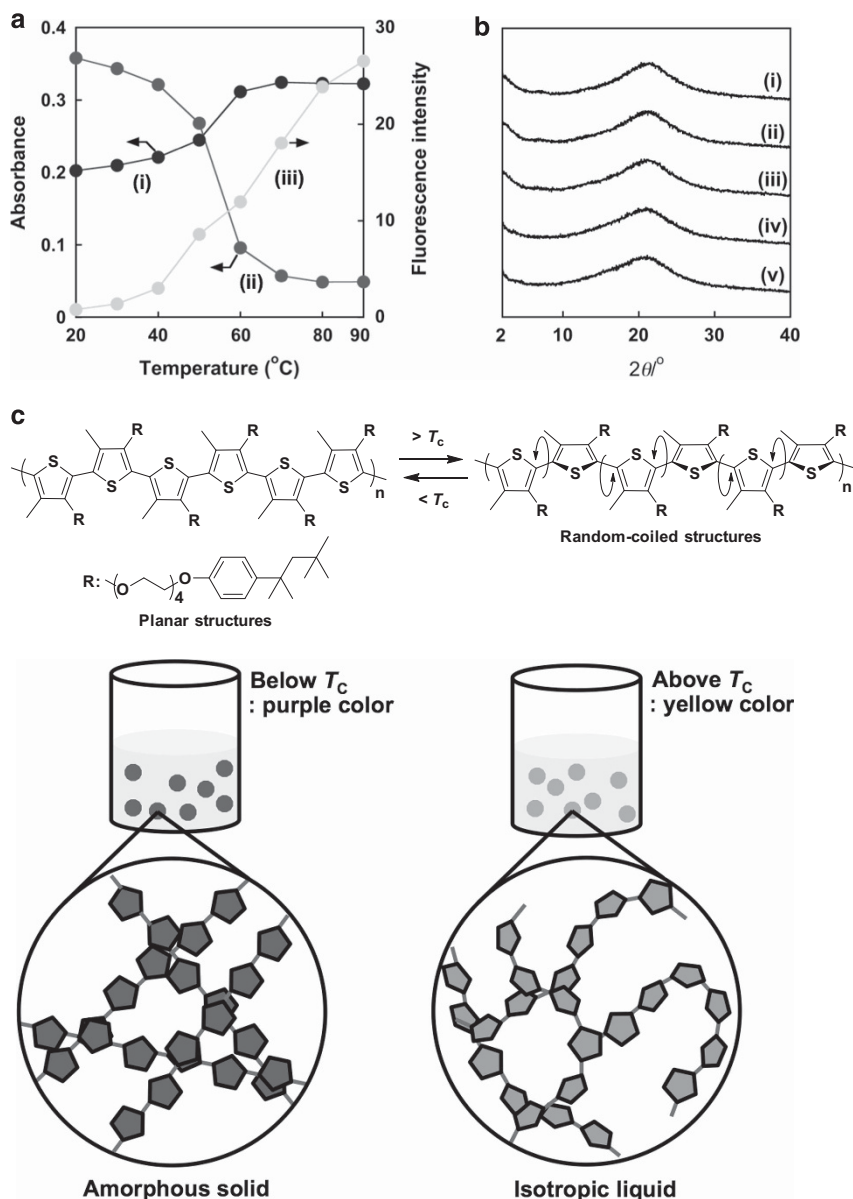


**Figure 6** (a) Changes in the absorption and fluorescence intensity of **PMTPT** nanoparticles in THF:H<sub>2</sub>O=2:98 (v/v) between 20 and 90 °C. Monitoring wavelength: absorbance at 431 nm (i) and 598 nm (ii); fluorescence intensity at 545 nm (iii). (b) XRD patterns of **PMTPT** powder obtained at (i) –30 °C, (ii) 10 °C, (iii) 40 °C, (iv) 80 °C and (v) 120 °C. (c) Schematic illustration of the thermochromic behavior of the **PMTPT** nanoparticles in aqueous media. THF, tetrahydrofuran; XRD, X-ray diffraction.

negative with the increasing water concentration. These results indicate that the size of the **PMTPT** nanoparticles is affected by the change in the aggregation structure in aqueous media with different solvent compositions. **PMTPT** consists of conjugated thiophene rings with hydrophilic oligo(ethylene oxide) side chains. When the water concentration is high, the conjugated thiophene unit tends to undergo self-assembled aggregation with the terminal phenyl group inside the nanoparticle because of its hydrophobicity. Effective hydrophobic aggregation results in  $\pi$ - $\pi$  packing, providing a smaller particle size as the water content increases. In contrast, miscible behavior is observed between the thiophene units and THF when the concentration of water is low. This miscibility may cause the particle size to increase, resulting from the insertion of solvent into the nanoparticles. The absorption spectra of the **PMTPT** nanoparticles in

THF:H<sub>2</sub>O=75:25 (v/v) resembled those of the **PMTPT** solution in anhydrous THF (Supplementary Figure S5). A yellow dispersion is obtained in both cases because the polythiophene units adopt a random coil conformation in the nanoparticles.

We also investigated the solvatochromic behavior of **PMTPT** in THF/EtOH mixtures (Supplementary Figure S6). The change of the absorption spectra of **PMTPT** in THF/EtOH mixtures was similar to that in THF/H<sub>2</sub>O mixtures (Supplementary Figure S6A). Unfortunately, the nanoparticles aggregated as the concentration of EtOH increased, as evidenced by TEM (Supplementary Figure S6B). Several nanoparticles gathered in the solution, leading to the formation of large aggregated particles. An increase in particle size was also revealed by DLS. An average size of 1474 nm with a polydispersity index of 0.25 was obtained at THF:EtOH=2:98 (v/v) (Supplementary



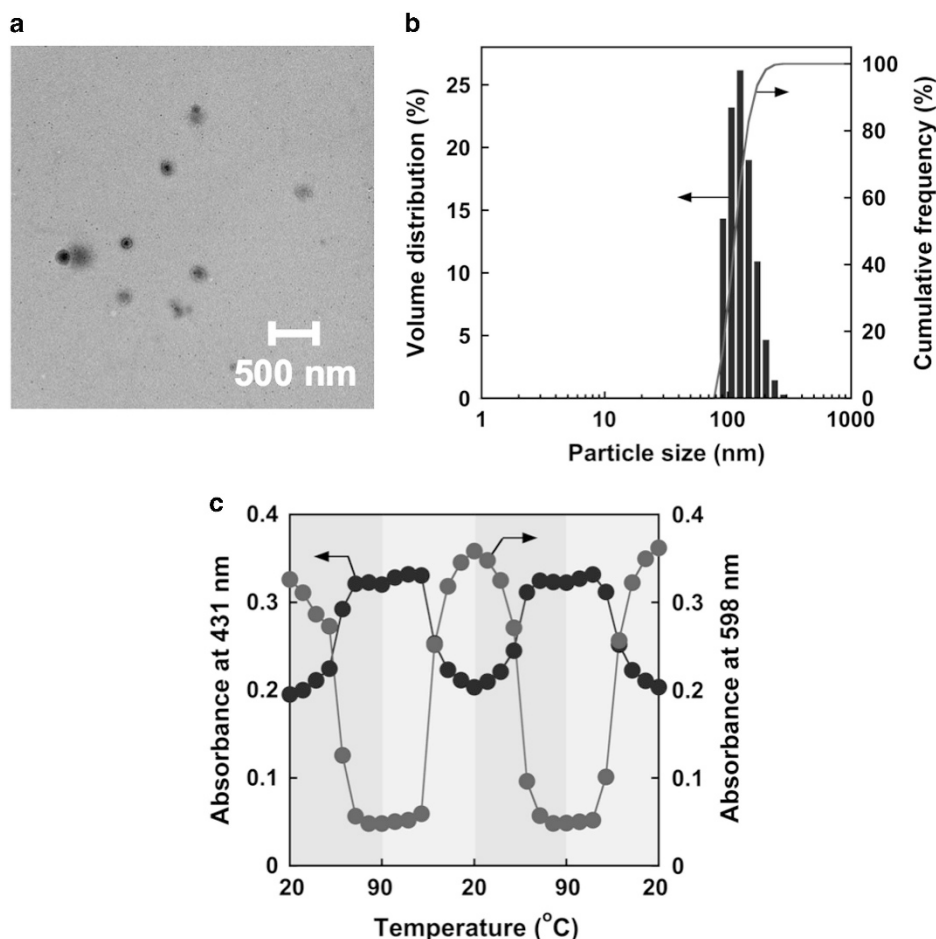


**Figure 7** (a) TEM image of **PMTPT** nanoparticles at 25 °C after thermal treatment. After cooling from 90 °C, the sample was prepared by casting the resultant solution in THF:H<sub>2</sub>O=2:98 (v/v) onto a TEM grid. (b) Size distribution of the thermally treated **PMTPT** nanoparticles. (c) Changes in absorbance at 431 nm and 598 nm of the **PMTPT** nanoparticles upon thermal cycling between 20 and 90 °C. TEM, transmission electron microscopy; THF, tetrahydrofuran.

Figure S6C). In contrast to the case in the THF/water mixtures (Figure 3b), large aggregated particles with an average size of over 10  $\mu\text{m}$  were observed in THF/EtOH. Moreover, the negative  $\zeta$  value of **PMTPT** in THF:EtOH=2:98 (v/v) ( $-25.3\text{ mV}$ ) was smaller than that in THF:H<sub>2</sub>O=2:98 (v/v) ( $-66.6\text{ mV}$ ). These results suggest that the instability of the particles in the THF/EtOH mixtures was caused by the lower electrostatic repulsion compared with that in THF/H<sub>2</sub>O.

#### Thermochromic behavior

Figure 5a and Supplementary Figure S8B show the change in color of the **PMTPT** nanoparticles in THF:H<sub>2</sub>O=2:98 (v/v) between 20 and 90 °C. The dispersion clearly changed from violet to yellow as the temperature increased. Conversely, when the solution temperature decreased from 90 to 20 °C, the yellow solution successfully reverted to its initial violet. The color of the **PMTPT** nanoparticles in aqueous media was investigated by the change of their absorption spectra with temperature (Figure 5b-(i)). As mentioned above, the absorbance of  $\lambda_{\text{max}}$  at 545 and 598 nm corresponding to the planar conformation of the **PMTPT** backbone decreased with rising temperature. In contrast, the absorbance at 431 nm corresponding to the random coil conformation of the main chain of **PMTPT** increased with rising temperature. The fluorescence spectra of the **PMTPT** nanoparticles in aqueous media also changed with the temperature because of

the thermally induced modulation of the molecular conformation of the polymer main chain (Figure 5b-(ii)). The maximum fluorescence intensity at 545 nm at 90 °C was 35 times higher than that at 20 °C. With increasing temperature, the molecular conformation changes from the planar structure to the random coil one, leading to suppression of the fluorescence quenching.

To clarify the temperature modulation of the conjugated structure in **PMTPT**, the dependence of the absorbance and fluorescence intensity on the temperature was monitored (Figure 6a). The molecular conformation in the **PMTPT** nanoparticles changed dramatically near the  $T_c$  of **PMTPT** of 60 °C. The absorbance of  $\lambda_{\text{max}}$  at 598 nm corresponding to the vibronic band of the  $\pi-\pi^*$  transition in the planar structure decreased substantially in the temperature range from 50 to 60 °C. In contrast, increases in the absorbance of  $\lambda_{\text{max}}$  at 431 nm and in the fluorescence intensity at 545 nm in this temperature range indicated the transformation of the conjugated polymer chain from the planar structure to the random coil. We also found that heating led to shifted isosbestic points around  $T_c$  in the absorption spectra (Figure 5b-(i)). The cooling profile was similar to the heating profile (Supplementary Figure S7), but spectral hysteresis was observed. Such hysteresis mainly originated from the order–disorder transition from planar to nonplanar of the thiophene units with different  $T_c$  values. In the DSC profile,  $T_c$  was 60 °C upon heating, as mentioned above. In contrast, an exothermic event at

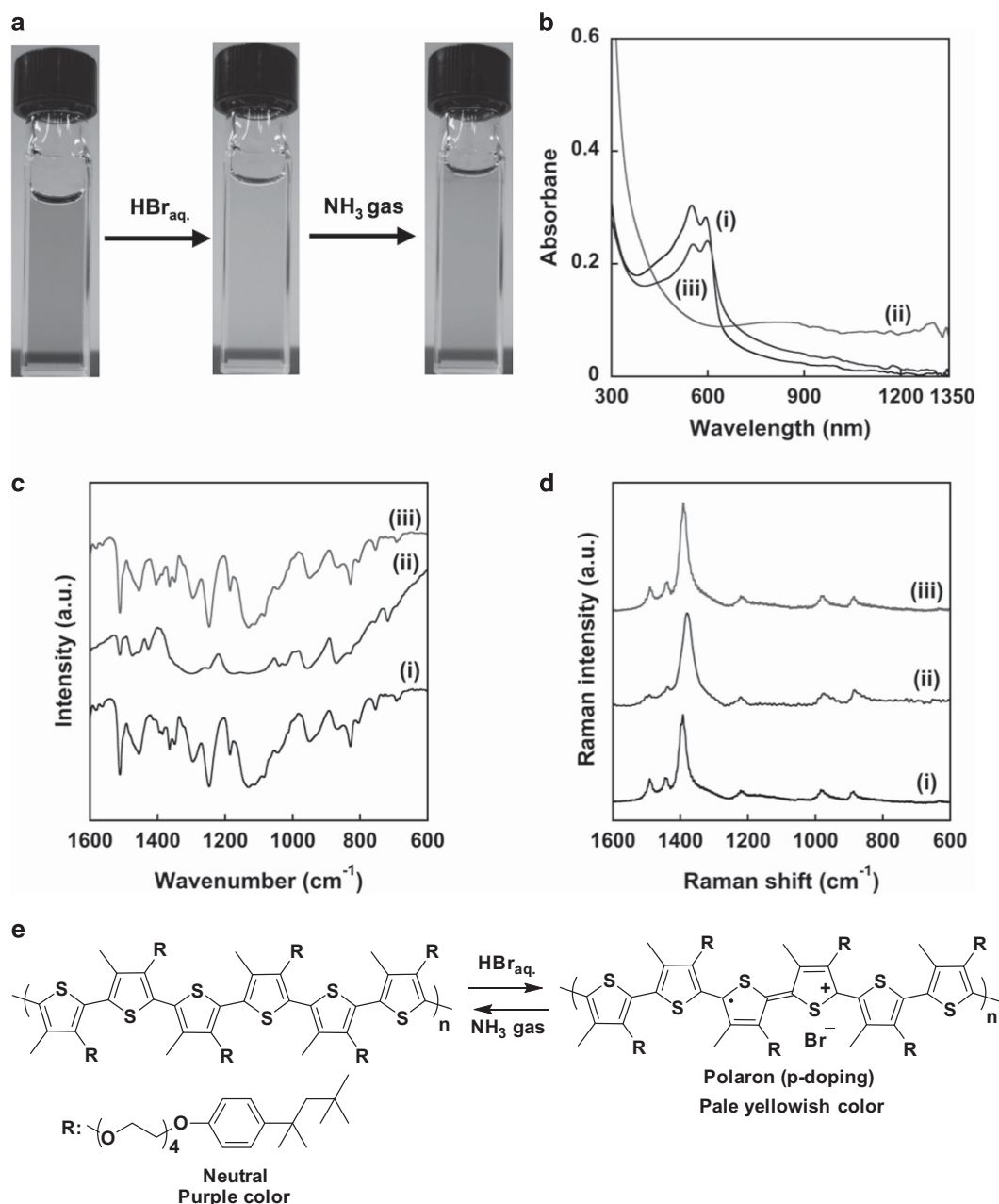


**Figure 8** (a) Halochromic behavior of **PMTPT** nanoparticles in  $\text{THF}:\text{H}_2\text{O}=2:98$  (v/v), demonstrated using hydrobromic acid ( $\text{HBr}_{\text{aq.}}$ ) and ammonia gas. (b) Change in absorption spectra of the **PMTPT** nanoparticles in aqueous media (i) before treatment, (ii) after the addition of  $\text{HBr}_{\text{aq.}}$ , and (iii) after the addition of ammonia gas. (c) FTIR and (d) Raman spectra of the **PMTPT** nanoparticles: (i) pristine sample, (ii) after soaking in  $\text{HBr}_{\text{aq.}}$ , and (iii) after bubbling with ammonia gas. (e) Schematic illustration of chemical doping in **PMTPT**. FTIR, Fourier transform infrared; THF, tetrahydrofuran.

a  $T_c$  of  $42^\circ\text{C}$  with a  $\Delta H$  of  $6.2\text{ kJ mol}^{-1}$  was obtained upon cooling (Supplementary Figure S2B). This discontinuous chromic response was also observed for polythiophene derivatives containing oligo (oxyethylene) units in the solid state.<sup>34</sup>

The morphology of **PMTPT** at the molecular level was investigated by X-ray diffraction. The X-ray diffraction patterns of the **PMTPT** powder showed only a broad halo, consistent with no crystalline nature below and above  $T_c$  (Figure 6b). Judging from its DSC profiles (Supplementary Figure S2B) and X-ray diffraction patterns, **PMTPT** possesses different morphologies in the temperature range between 20 and  $90^\circ\text{C}$ : an amorphous solid and isotropic liquid are

observed at 20–60 and 60– $90^\circ\text{C}$ , respectively. From these spectroscopic and morphological results, we conclude that the thermochromic behavior of the nanoparticles mainly originated from the varying molecular conformations of the conjugated thiophene units in the different morphologies (Figure 6c). Below  $T_c$ , the **PMTPT** nanoparticles were a purple amorphous solid in which the main chains adopted a planar structure. The conformation of the conjugated thiophene units of **PMTPT** gradually fluctuated upon approaching  $T_c$ . Above  $T_c$ , yellow nanoparticles composed of an isotropic liquid with a random coil structure are obtained.

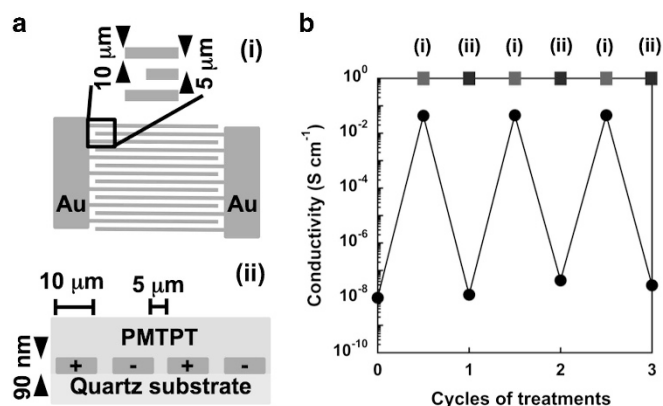


**Figure 9** (a) Schematic illustrations of the interdigitated gold electrodes and sample configuration. (i) Top view of the electrodes and (ii) side view of the sample configuration. (b) Change in the electrical conductivity of **PMTPT** after dipping in hydrobromic acid for 5 min (i) and after exposure to ammonia gas for 20 s (ii).

The structural stability and reversibility of the thermochromic response of the nanoparticles were also evaluated using TEM and DLS analyses. The size of the **PMTPT** nanoparticles in THF:H<sub>2</sub>O=2:98 (v/v) after the thermal treatment, estimated from the TEM image, was 139 nm (Figure 7a). Comparison with the TEM image in Figure 3a shows that the particle size and structure remained unchanged following the thermal treatment. The DLS results revealed that the average particle size and polydispersity index of the thermally treated nanoparticles were 150 nm and 0.05, respectively (Figure 7b). We found that the  $\zeta$  of the nanoparticles in THF:H<sub>2</sub>O=2:98 (v/v) after heating to 90 °C (−66.8 mV) was almost the same as that before the thermal treatment (−66.6 mV). Figure 7c shows the change in the absorbance of the **PMTPT** nanoparticles in THF:H<sub>2</sub>O=2:98 (v/v) upon repeated cycling between 20 and 90 °C. The absorbance peaks at 431 and 598 nm corresponding to the  $\pi$ – $\pi^*$  transitions in the random coil and planar structures changed during cycling, indicating a reversible transformation between the amorphous solid and isotropic liquid nanoparticles in aqueous media.

### Halochromic behavior

Figure 8a and Supplementary Figure S8C show the color change of the **PMTPT** nanoparticles in THF:H<sub>2</sub>O=2:98 (v/v) upon chemical treatment. When hydrobromic acid (47% in water, 0.2 ml, 1.8 mmol) was added to an aqueous dispersion of the nanoparticles (3 ml, 2.5 mg l<sup>-1</sup>), a pale yellowish solution was obtained within 5 min. The initial purple solution was regenerated by bubbling with ammonia gas (20 ml min<sup>-1</sup>) for 2 min.

Spectroscopic results indicated that the color change of the **PMTPT** nanoparticles was essentially reversible (Figure 8b). After the addition of hydrobromic acid, the absorbance of  $\lambda_{\max}$  at 552 and 598 nm corresponding to the  $\pi$ – $\pi^*$  transition of the planar polythiophene structure decreased, and a broad peak appeared in the near-infrared region at approximately 855 nm (Figure 8b-(ii)). The initial absorption spectra returned after adding ammonia gas (Figure 8b-(iii)); the decrease in absorbance was due to change in the concentration of the aqueous solution after addition of hydrobromic acid. We assumed that this change in the absorption spectra might be caused by the generation of polarons by the chemical doping of the thiophene units with hydrobromic acid.

The formation of polarons in the **PMTPT** nanoparticles was examined by Fourier transform infrared and Raman spectroscopies (Figures 8c and d). Specific bands corresponding to antisymmetric and symmetric stretching modes of the thiophene rings at 1511 and 1455 cm<sup>-1</sup>, respectively, and an asymmetric C–O stretching band of the oligo(ethylene oxide) group at 1129 cm<sup>-1</sup> were observed for the pristine film (Figure 8c-(i)). After the addition of hydrobromic acid to the dispersion, the resulting cast film exhibited a sharp decrease in the intensity of the ring-stretching modes. In addition, new broad bands were observed at 1172 and 1039 cm<sup>-1</sup>, which are consistent with the polarons of polythiophene derivatives such as poly(3-methylthiophene) (1165 and 976 cm<sup>-1</sup>)<sup>35</sup> and poly(3-hexylthiophene) (1129 and 1068 cm<sup>-1</sup>).<sup>36,37</sup> Because the corresponding bands overlapped with the asymmetric C–O stretching bands of the oligo(ethylene oxide) groups, the polarons of **PMTPT** could not be detected clearly. The specific stretching bands of the thiophene rings were recovered after bubbling ammonia gas through the solution treated with hydrobromic acid (Figure 8c-(iii)).

The Raman spectra clearly exhibited polaron formation. The bands at 1490 and 1443 cm<sup>-1</sup> were assigned to the antisymmetric and symmetric stretching bands of the thiophene rings (Figure 8d-i), respectively, and the band at 1391 cm<sup>-1</sup> was attributed to symmetric C–C stretching deformation.<sup>38</sup> After the hydrobromic acid treatment, the Raman intensity of these aromatic bands weakened, and the C–C stretching mode originating from the positive polaron was observed at 1380 cm<sup>-1</sup> (Figure 8d-(ii)).<sup>36</sup> The initial spectra were regenerated by bubbling ammonia gas through the hydrobromic acid-treated solution (Figure 8d-(iii)).

We concluded that the color change of the **PMTPT** nanoparticles was derived from halochromic responses induced by the chemical doping of the conjugated thiophene units (Figure 8e). The addition of hydrobromic acid in aqueous media led to almost colorless nanoparticles composed of p-doped **PMTPT**. The initial purple **PMTPT** nanoparticles were observed after the addition of a reducing reagent (ammonia gas), resulting from the dedoping of the p-doped **PMTPT** (Figures 8a and b-(iii)). After the formation of neutral **PMTPT**, the hydrobromic acid reacted with ammonia gas to yield water-soluble ammonium bromide.

We anticipated that the halochromic reaction of **PMTPT** would change its electrical conductivity ( $\sigma$ ). To evaluate this hypothesis, the alternating p-doping and dedoping of **PMTPT** in the solid state was performed. A sample was prepared by casting **PMTPT** solution onto an interdigitated gold electrode (Figure 9a). The estimation of the  $\sigma$  of the solid-state samples is described in the Supplementary Information. Figure 9b shows the change in  $\sigma$  of the sample upon immersion in hydrobromic acid (0.1 ml, 0.89 mmol) and exposure to ammonia gas (20 ml min<sup>-1</sup>) repeatedly. Neutral **PMTPT** exhibited a low  $\sigma$  of  $1.0 \times 10^{-8}$  S cm<sup>-1</sup>. The change in  $\sigma$  after immersion in hydrobromic acid was nearly 10<sup>6</sup>, and its value was immediately reverted by ammonia gas treatment. Reversible changes in the  $\sigma$  could be achieved by the chemical doping of **PMTPT** in the solid state.

### CONCLUSIONS

We successfully demonstrated that a polythiophene derivative (**PMTPT**) formed stable nanoparticles in aqueous media that displayed reversible multichromic behavior. The solvatochromism of the nanoparticles was observed when the concentration of water in the solution was increased. The nanoparticle size gradually decreased upon increasing the concentration of water. The resultant nanoparticles with an average diameter of 170 nm and a large zeta potential of −66.6 mV formed an aqueous dispersion that remained stable even after



8 months. The thermochromic responses of the PMTPT nanoparticles were derived from the morphological changes between an amorphous solid and isotropic liquid, and the color changes originated from the different molecular conformations of the conjugated main chain, including planar and random coil polymer structures. The halochromic behavior of the PMTPT nanoparticles was achieved by the p-doping and dedoping of the conjugated thiophene units. Chemical doping caused the conductivity of the solid-state nanoparticle samples to change.

## CONFLICT OF INTEREST

The authors declare no conflict of interest.

## ACKNOWLEDGEMENTS

We thank Dr Daisuke Hashizume and Ms Tomoka Kikitsu of the Materials Characterization Support Unit, RIKEN Center for Emergent Matter Science (CEMS), for the X-ray diffraction and TEM measurements and for their valuable comments and discussion. We also thank Professor Yu Nagase and Mr Tomoki Mimura of Tokai University for the GPC measurements and their comments. We acknowledge Dr Keisuke Tajima of the Emergent Functional Polymers Research Team, RIKEN CEMS, for the electrical conductivity measurements. We also thank Dr Zhaomin Hou and Dr Masayoshi Nishiura of the Organometallic Chemistry Laboratory, RIKEN, for the thermogravimetric analysis and DSC measurements. We thank Mr Takeo Soejima of the Applicative Solution Laboratory Division, JASCO, for the Raman measurements and technical support. This work was partially supported by a Grant-in-Aid for Scientific Research (C) (No. 15K05639) to MK from the Ministry of Education, Culture, Sports, Science and Technology of Japan.

- 1 Thomas, S. W., Joly, G. D. & Swager, T. M. Chemical sensors based on amplifying fluorescent conjugated polymers. *Chem. Rev.* **107**, 1339–1386 (2007).
- 2 Hoeben, F. J. M., Jonkheijm, P., Meijer, E. W. & Schenning, A. P. H. J. About supramolecular assemblies of  $\pi$ -conjugated systems. *Chem. Rev.* **105**, 1491–1546 (2005).
- 3 Aida, T., Meijer, E. W. & Stupp, S. I. Functional supramolecular polymers. *Science* **335**, 813–817 (2012).
- 4 Stuart, M. A. C., Huck, W. T., Genzer, J., Müller, M., Ober, C., Stamm, M., Sukhorukov, G. B., Szleifer, I., Tsukruk, V. V., Urban, M., Winnik, F., Zauscher, S., Luzinov, I. & Minko, S. Emerging applications of stimuli-responsive polymer materials. *Nat. Mater.* **9**, 101–113 (2010).
- 5 Lee, J., Pyo, M., Lee, S. H., Kim, J., Ra, M., Kim, W. Y., Park, B. J., Lee, C. W. & Kim, J. M. Hydrochromic conjugated polymers for human sweat pore mapping. *Nat. Commun.* **5**, 3736 (2014).
- 6 Lee, J., Chang, H. T., An, H., Ahn, S., Shim, J. & Kim, J. M. A Protective Layer Approach to Solvatochromic Sensors. *Nat. Commun.* **4**, 2461 (2013).
- 7 Lee, E., Hammer, B., Kim, J. K., Page, Z., Emrick, T. & Hayward, R. C. Hierarchical helical assembly of conjugated poly(3-hexylthiophene)-block-poly(3-triethylene glycol thiophene) diblock copolymers. *J. Am. Chem. Soc.* **133**, 10390–10393 (2011).
- 8 Lévesque, I., Bazinet, P. & Roovers, J. Optical properties and dual electrical and ionic conductivity in poly(3-methylhexa(oxyethylene)oxy-4-methylthiophene). *Macromolecules* **33**, 2952–2957 (2000).
- 9 Turchetti, D. A., Domingues, R. A., Zanlorenzi, C., Nowacki, B., Atvars, T. D. Z. & Akcelrud, L. C. A photophysical interpretation of the thermochromism of a polyfluorene derivative-europium complex. *J. Phys. Chem. C* **118**, 30079–30086 (2014).
- 10 Richards, C. E. & Phillips, R. T. Solvatochromic effects on the photoinduced charge-transfer states in donor-acceptor substituted polydiethylfluorenes. *Chem. Phys. Chem.* **12**, 2831–2835 (2011).
- 11 Pecher, J. & Mecking, S. Nanoparticles of conjugated polymers. *Chem. Rev.* **110**, 6260–6279 (2010).
- 12 Tuncel, D. & Demir, H. V. Conjugated polymer nanoparticles. *Nanoscale* **2**, 484–494 (2010).
- 13 Ong, B. S., Wu, Y., Liu, P. & Gardner, S. Structurally ordered polythiophene nanoparticles for high-performance organic thin-film transistors. *Adv. Mater.* **17**, 1141–1144 (2005).
- 14 Palner, M., Pu, K., Shao, S. & Rao, J. Semiconducting polymer nanoparticles with persistent near-infrared luminescence for *in vivo* optical imaging. *Angew. Chem. Int. Ed.* **54**, 11477–11480 (2015).
- 15 Pu, K., Shuhendler, A. J., Jokerst, J. V., Mei, J., Gambhir, S. S., Bao, Z. & Rao, J. Semiconducting polymer nanoparticles as photoacoustic molecular imaging probes in living mice. *Nat. Nanotechnol.* **9**, 233–239 (2014).
- 16 Xiong, L., Shuhendler, A. J. & Rao, J. Self-luminescing BRET-FRET near-infrared dots for *in vivo* lymph-node mapping and tumour imaging. *Nat. Commun.* **3**, 1193 (2012).
- 17 Wu, C. & Chiu, D. T. Highly fluorescent semiconducting polymer dots for biology and medicine. *Angew. Chem. Int. Ed.* **52**, 3086–3109 (2013).
- 18 Moon, J. H., Mendez, E., Kim, Y. & Kaur, A. Conjugated polymer nanoparticles for small interfering RNA delivery. *Chem. Commun.* **47**, 8370–8372 (2011).
- 19 Das, S., Samanta, S., Chatterjee, D. P. & Nandi, A. K. Thermosensitive water-soluble poly(ethylene glycol)-based polythiophene graft copolymers. *J. Polym. Sci. Part A* **51**, 1417–1427 (2013).
- 20 Moon, J. H., Deans, R., Krueger, E. & Hancock, L. F. Capture and detection of a quencher labeled oligonucleotide by poly(phenylene ethynylene) particles. *Chem. Commun.* 104–105 (2003).
- 21 Brustolin, F., Goldoni, F., Meijer, E. W. & Sommerdijk, N. A. J. M. Highly ordered structures of amphiphilic polythiophenes in aqueous media. *Macromolecules* **35**, 1054–1059 (2002).
- 22 Gilbert, T. W., Sellar, T. L. & Badylak, S. F. Decellularization of tissues and organs. *Biomaterials* **27**, 3675–3683 (2006).
- 23 Garvalov, B. K., Foss, F., Henze, A. T., Bethani, I., Gräf-Höchst, S., Singh, D., Filatova, A., Dopeso, H., Seidel, S., Damm, M., Acker-Palmer, A. & Acker, T. PHD3 regulates EGFR internalization and signalling in tumours. *Nat. Commun.* **5**, 5577 (2014).
- 24 Wu, X., Liu, H., Liu, J., Haley, K. N., Treadway, J. A., Larson, J. P., Ge, N., Peale, F. & Bruchez, M. P. Immunofluorescent labeling of cancer marker Her2 and other cellular targets with semiconductor quantum dots. *Nat. Biotechnol.* **21**, 41–46 (2003).
- 25 Mei, J. & Bao, Z. Side chain engineering in solution-processable conjugated polymers. *Chem. Mater.* **26**, 604–615 (2014).
- 26 Chandler, D. Interfaces and the driving force of hydrophobic assembly. *Nature* **437**, 640–647 (2005).
- 27 Wu, C., Szymanski, C. & McNeill, J. Preparation and encapsulation of highly fluorescent conjugated polymer nanoparticles. *Langmuir* **22**, 2956–2960 (2006).
- 28 Qin, G. & Cai, C. Oxidative degradation of oligo(ethylene glycol)-terminated monolayers. *Chem. Commun.* 5112–5114 (2009).
- 29 Matthews, J. R., Goldoni, F., Schenning, A. P. H. J. & Meijer, E. W. Non-ionic polythiophenes: a non-aggregating folded structure in water. *Chem. Commun.* 5503–5505 (2005).
- 30 Crosby, G. A. & Demas, J. N. Measurement of photoluminescence quantum yields. *Review. J. Phys. Chem.* **75**, 991–1024 (1971).
- 31 Li, C., Numata, M., Bae, A. H., Sakurai, K. & Shinkai, S. Self-assembly of supramolecular chiral insulated molecular wire. *J. Am. Chem. Soc.* **127**, 4548–4549 (2005).
- 32 Lai, S. K., O'Hanlon, D. E., Harrold, S., Man, S. T., Wang, Y. Y., Cone, R. & Hanes, J. Rapid transport of large polymeric nanoparticles in fresh undiluted human mucus. *Proc. Natl. Acad. Sci. USA* **104**, 1482–1487 (2007).
- 33 Chen, K., Liang, D., Tian, J., Shi, L. & Zhao, H. In-situ polymerization at the interfaces of micelles: a 'grafting from' method to prepare micelles with mixed coronal chains. *J. Phys. Chem. B* **112**, 12612–12617 (2008).
- 34 Lévesque, I. & Leclerc, M. Ionochromic and thermochromic phenomena in a regioregular polythiophene derivative bearing oligo(oxyethylene) side chains. *Chem. Mater.* **8**, 2843–2849 (1996).
- 35 Kim, Y. H., Hotta, S. & Heeger, A. J. Infrared photoexcitation and doping studies of poly(3-methylthienylene). *Phys. Rev. B* **36**, 7486–7490 (1987).
- 36 Yamamoto, J. & Furukawa, Y. Electronic and vibrational spectra of positive polarons and bipolarons in regioregular poly(3-hexylthiophene) doped with ferric chloride. *J. Phys. Chem. B* **119**, 4788–4794 (2015).
- 37 Kim, Y. H., Spiegel, D., Hotta, S. & Heeger, A. J. Photoexcitation and doping studies of poly(3-hexylthienylene). *Phys. Rev. B* **38**, 5490–5495 (1988).
- 38 Pron, A., Louarn, G., Lapkowski, M., Zagorska, M., Glowczy-Zubek, J. & Lefrant, S. 'In situ' Raman spectroelectrochemical studies of poly(3,3'-dibutoxy-2,2'-bithiophene). *Macromolecules* **28**, 4644–4649 (1995).

Supplementary Information accompanies the paper on Polymer Journal website (<http://www.nature.com/pj>)